

Effect of radiation trapping on the polarization of an optically pumped alkali-metal vapor

D. Tupa, L. W. Anderson, D. L. Huber, and J. E. Lawler
Department of Physics, University of Wisconsin, Madison, Wisconsin 53706
 (Received 25 July 1985)

Calculations are presented of the limitations imposed by radiation trapping on the electron spin polarization produced in an alkali-metal vapor by optical pumping in a large magnetic field. It is found that electron spin polarizations of 90% are possible with Na densities up to 10^{19} atoms/m³ and ground-level relaxation times of 150 μ s in a large magnetic field using a cylindrical geometry of radius 7.5×10^{-3} m.

I. INTRODUCTION

The use of laser optical pumping to produce a polarized alkali-metal vapor is of current interest. An important effect in the optical pumping of alkali-metal vapors is the trapping of the pumping light.¹ Trapping occurs when the alkali-metal vapor is sufficiently dense that multiple scattering of the light is important for one or more radiative decay branches of the vapor. This paper reports the first calculations of the effect of radiation trapping on the electron-spin polarization produced in an alkali-metal vapor by optical pumping.

Previous radiation-trapping calculations have treated the case where the ground level is unpolarized.²⁻⁶ In an optically pumped vapor the populations of the individual states in the ground level are unequal. Radiation-trapping calculations in such a vapor, therefore, must include the polarization and angular dependence of the emitted and reabsorbed resonance radiation. The situation where the ground level is polarized is consequently more complicated than that where the ground level is unpolarized. Our calculations give, for a cylindrical geometry, the ground-state polarization for optically pumped alkali-metal vapors in a large magnetic field as a function of the optical pumping light intensity, the ground-level relaxation time, and the alkali-metal density.

II. METHOD OF CALCULATIONS

We report calculations of the effects of radiation trapping for an "idealized alkali-metal" atom with electron spin S of $\frac{1}{2}$ and with zero nuclear spin. There is no real

alkali-metal atom with zero nuclear spin. We discuss the optical pumping of the idealized alkali-metal atom using σ^- polarized light with a wavelength corresponding to absorption from the $^2S_{1/2}$, $m = \frac{1}{2}$ state in the ground level to the $^2P_{1/2}$, $m = -\frac{1}{2}$ state in the lowest-lying excited level. Figure 1 shows the relevant energy levels. We label the states as follows: The $^2S_{1/2}$, $m = -\frac{1}{2}$ state is labeled 1, the $^2S_{1/2}$, $m = \frac{1}{2}$ state is labeled 2, the $^2P_{1/2}$, $m = -\frac{1}{2}$ state is labeled 3, and the $^2P_{1/2}$, $m = \frac{1}{2}$ state is labeled 4. We denote by λ_{ij} the wavelength at line center for the absorption from the ground state to the excited state. For our calculations we assume the optical pumping is carried out in a magnetic field large enough that the wavelengths λ_{13} , λ_{14} , λ_{23} , and λ_{24} are separated by several Doppler linewidths so that the lines are completely isolated; light with a wavelength corresponding to one absorption line does not result in absorption by another line. We also assume that collisions of alkali atoms with other atoms or with walls result in a relaxation between ground states 1 and 2 but do not result in appreciable excitation transfer between the excited states 3 and 4. Under these conditions state 4 plays no role, and only states 1, 2, and 3 are populated.

We calculate the populations of states 1, 2, and 3 as follows. The laser light at wavelength λ_{23} excites atoms from state 2 to state 3, and stimulates atoms in state 3 to emit and return to state 2. Atoms in state 3 may decay spontaneously to either states 1 or 2, and the spontaneously emitted photons can be trapped. If the population of atoms in states 1 and 2 are unequal, collisional relaxation occurs between these states. These processes are described by the following rate equations:

$$\begin{aligned} \frac{dn_2(\mathbf{r},t)}{dt} = & -\frac{\lambda_{23}^2}{4\pi} A_3 \left[\int \frac{I_{\bar{\nu}}}{h\bar{\nu}} g(\nu_{23}-\bar{\nu}) d\bar{\nu} \right] [n_2(\mathbf{r},t) - n_3(\mathbf{r},t)] + A_{32}n_3(\mathbf{r},t) - \frac{n_2(\mathbf{r},t) - n_1(\mathbf{r},t)}{T_1} \\ & - \left[\int d^3r' d\nu n_3(\mathbf{r}',t) \frac{A_3(1+\cos^2\theta)}{8\pi|\mathbf{r}-\mathbf{r}'|^2} g(\nu-\nu_{23}) \right. \\ & \quad \times \exp \left[-\frac{\lambda_{23}^2}{8\pi} A_3(1+\cos^2\theta) g(\nu-\nu_{23}) \int_0^{|\mathbf{r}-\mathbf{r}'|} (n_2-n_3) d\rho \right] \\ & \quad \left. \times \frac{\lambda_{23}^2}{8\pi} A_3(1+\cos^2\theta) g(\nu-\nu_{23}) [n_2(\mathbf{r},t) - n_3(\mathbf{r},t)] \right], \end{aligned} \tag{1}$$

$$\frac{dn_1(\mathbf{r},t)}{dt} = A_{31}n_3(\mathbf{r},t) + \frac{n_2(\mathbf{r},t) - n_1(\mathbf{r},t)}{T_1} - \left[\int d^3r' d\nu n_3(\mathbf{r}',t) \frac{A_3 \sin^2\theta}{8\pi |\mathbf{r}-\mathbf{r}'|^2} g(\nu-\nu_{13}) \exp \left[-\frac{\lambda_{13}^2}{8\pi} A_3 \sin^2\theta g(\nu-\nu_{13}) \int_0^{|\mathbf{r}-\mathbf{r}'|} (n_1 - n_3) d\rho \right] \times \frac{\lambda_{13}^2}{8\pi} A_3 \sin^2\theta g(\nu-\nu_{13}) [n_1(\mathbf{r},t) - n_3(\mathbf{r},t)] \right], \quad (2)$$

and

$$N(\mathbf{r},t) = n_1(\mathbf{r},t) + n_2(\mathbf{r},t) + n_3(\mathbf{r},t). \quad (3)$$

Equation (3) expresses the total atomic density $N(\mathbf{r},t)$ at position \mathbf{r} and time t as the sum of the atomic densities in states 1, 2, and 3. This makes explicit the assumption that collisions do not populate state 4 or other higher states. The Einstein A coefficients between state 3 and states 1 and 2 are, respectively, A_{31} and A_{32} . Thus $A_3 = A_{31} + A_{32}$, where A_3^{-1} is radiative lifetime of state 3. For the decay from a $^2P_{1/2}$ level to a $^2S_{1/2}$ level, $A_{31} = A_3/3$ and $A_{32} = 2A_3/3$. The relaxation time between states 1 and 2 is T_1 . The intensity per unit frequency of the light source used for the optical pumping is $I_{\bar{\nu}}$; $\bar{\nu}$ is the frequency of the pumping light. The optical absorption cross section for state 2 to state 3 for σ^- light of frequency $\bar{\nu}$ is $\lambda_{23}^2 g(\nu_{23} - \bar{\nu}) A_3 / 4\pi$. The angle between $\mathbf{r} - \mathbf{r}'$ and the direction of the magnetic field is θ . We denote frequency by ν so that $\nu_{ij} = c/\lambda_{ij}$.

The first term on the right side of Eq. (1) represents the absorption and stimulated emission due to the pumping light. The second term represents the spontaneous radiative decay from state 3 to state 2 and the third term represents the ground-state relaxation. The final term in

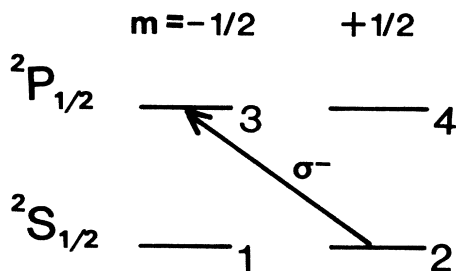


FIG. 1. Energy levels of the idealized alkali-metal atom. Optical pumping with σ^- light excites the transition 2 \rightarrow 3 as shown.

Eq. (1) represents the radiation trapping and describes three processes. The first process is the radiative decay of atoms in state 3 at position \mathbf{r}' to state 2 with the appropriate angular distribution and with a normalized line shape $g(\nu - \nu_{23})$, where ν is the frequency of the emitted radiation. For our calculations we take $g(\nu - \nu_{23})$ to be the normalized Doppler line shape

$$g(\nu - \nu_{23}) = \left[\frac{Mc^2}{2\pi kT\nu_{23}^2} \right]^{1/2} \exp \left[- \left[\frac{\nu - \nu_{23}}{\nu_{23}} \right]^2 \frac{Mc^2}{2kT} \right].$$

The second process in the radiation-trapping terms is the absorption of light as it passes from position \mathbf{r}' to position \mathbf{r} . The line integral of the population difference along the path from \mathbf{r}' to \mathbf{r} is $\int (n_2 - n_3) d\rho$, where ρ is the element of length. The final process is the absorption of light at position \mathbf{r} . The terms in Eq. (2) have corresponding interpretations.

Equations (1)–(3) are very complex. We make a number of assumptions in their solution. First we assume that the intensity of the pumping light is constant rather than an exponentially decreasing function of position as the light propagates through the alkali-metal vapor, and we assume that the light source is broad compared to the absorption line so that it completely covers the line with constant intensity per unit frequency $I_{\bar{\nu}}$. We assume the alkali-metal vapor is confined to a cylindrical volume of radius R having a length very large compared to R . Third, we assume that scattered photons reaching $r = R$ are completely absorbed, i.e., the target walls are nonreflective. Fourth, and most importantly, we assume that the atomic densities n_1 , n_2 , and n_3 are independent of the position in the cylindrical volume. We discuss the uncertainty due to these assumptions later in this paper.

Since n_1 , n_2 , and n_3 are assumed to be independent of position, we need to solve for n_1 , n_2 , and n_3 at only one location in order to obtain n_1 , n_2 , and n_3 everywhere. We solve for these densities at the center of the long cylindrical volume. We call this location $\mathbf{r} = 0$. By using our assumptions, Eqs. (1)–(3) can be rewritten as

$$\begin{aligned} \frac{dn_2}{dt} = & -\frac{I_{\bar{\nu}}}{h\nu_{23}} \frac{\lambda_{23}^2}{4\pi} A_3(n_2 - n_3) + A_{32}n_3 - \frac{n_2 - n_1}{T_1} \\ & - A_3n_3 \left[\int d^3r' d\nu \frac{1 + \cos^2\theta}{8\pi r'^2} g(\nu - \nu_{23}) \exp \left[-\frac{\lambda_{23}^2}{8\pi} A_3(1 + \cos^2\theta)g(\nu - \nu_{23})(n_2 - n_3)r' \right] \right. \\ & \left. \times \frac{\lambda_{23}^2}{8\pi} A_3(1 + \cos^2\theta)g(\nu - \nu_{23})(n_2 - n_3) \right], \end{aligned} \quad (4)$$

$$\begin{aligned} \frac{dn_1}{dt} = & A_{31}n_3 + \frac{n_2 - n_1}{T_1} - A_3n_3 \left[\int d^3r' d\nu \frac{\sin^2\theta}{8\pi r'^2} g(\nu - \nu_{13}) \exp \left[-\frac{\lambda_{13}^2}{8\pi} A_3 \sin^2\theta g(\nu - \nu_{13})(n_1 - n_3)r' \right] \right. \\ & \left. \times \frac{\lambda_{13}^2}{8\pi} A_3 \sin^2\theta g(\nu - \nu_{13})(n_1 - n_3) \right], \end{aligned} \quad (5)$$

and

$$N = n_1 + n_2 + n_3. \quad (6)$$

The atomic density N is a constant independent of position and depends only on the temperature. In Eqs. (4) and (5) the integral of

$$d^3r' = 2\pi r'^2 dr' \sin\theta d\theta$$

is over the cylindrical volume of the alkali-metal vapor. The distance from $r=0$, the center of the cylinder, to r' is r' . The angle between $r-r'$ and the z axis is θ . We take the magnetic field along the z axis so that this θ agrees with our earlier definition. The integral over frequency is from $\nu=0$ to $\nu=\infty$.

The integrals in the radiation-trapping terms are evaluated numerically. We first perform the integration over frequency. This integral is evaluated using Hermite integration, in which an integral of the form $\int_{-\infty}^{\infty} e^{-x^2} F(x) dx$ is approximated as

$$\int_{-\infty}^{\infty} e^{-x^2} F(x) dx = \sum_{i=1}^n \omega_i F(\chi_i).$$

The values χ_i , which are the zeros of the Hermite polynomials, and the weighting factors ω_i are given by Abramowitz and Stegun.⁷ We use terms up to $n=20$ in our integration. In the integration over frequency, we let $x = [(\nu - \nu_0)/\nu_0](Mc^2/2kT)^{1/2}$ and we extend the integral over x from $-\infty$ to $+\infty$ rather than from $-(Mc^2/2kT)^{1/2}$ to ∞ . After Eqs. (4) and (5) have been integrated over frequency, we obtain

$$\begin{aligned} \frac{dn_2}{dt} = & -\frac{I_{\bar{\nu}}}{h\nu_{23}} \frac{\lambda_{23}^2}{4\pi} A_3(n_2 - n_3) + A_{32}n_3 - \frac{n_2 - n_1}{T_1} \\ & - (A_3n_3/4\sqrt{\pi}) \int_{\theta=0}^{\pi} \int_{r'=0}^{R/\sin\theta} \sum_i^{n=20} \omega_i (1 + \cos^2\theta)^2 (n_2 - n_3) \gamma_i \exp[-(n_2 - n_3)(1 + \cos^2\theta)\gamma_i r'] dr' \sin\theta d\theta, \end{aligned}$$

where

$$\gamma_i = \frac{\lambda_{23}^2}{8\pi} A_3 \left[\frac{Mc^2}{2\pi k T \nu_{23}^2} \right]^{1/2} e^{-x_i^2}, \quad (8)$$

and

$$\frac{dn_1}{dt} = A_{31}n_3 + \frac{n_2 - n_1}{T_1} - (A_3n_3/4\sqrt{\pi}) \int_{\theta=0}^{\pi} \int_{r'=0}^{R/\sin\theta} \sum_i^{n=20} \omega_i \sin^4\theta (n_1 - n_3) \gamma'_i \exp[-(n_1 - n_3) \sin^2\theta \gamma'_i r'] dr' \sin\theta d\theta, \quad (9)$$

where

$$\gamma'_i = \frac{\lambda_{13}^2}{8\pi} A_3 \left[\frac{Mc^2}{2\pi k T \nu_{13}^2} \right]^{1/2} e^{-x_i^2}. \quad (10)$$

The integration over r' can be carried out exactly, yielding

$$\frac{dn_2}{dt} = -\frac{I_{\bar{\nu}}}{h\nu_{23}} \frac{\lambda_{23}^2}{4\pi} A_3(n_2 - n_3) + A_{32}n_3 - \frac{n_2 - n_1}{T_1} - (A_3n_3/4\sqrt{\pi}) \sum_i \omega_i \int_0^\pi \{1 - \exp[-(1 + \cos^2\theta)(n_2 - n_3)\gamma_i R / \sin\theta]\} (1 + \cos^2\theta) \sin\theta d\theta \tag{11}$$

and

$$\frac{dn_1}{dt} = A_{31}n_3 + \frac{n_2 - n_1}{T_1} - (A_3n_3/4\sqrt{\pi}) \sum_i \omega_i \int_0^\pi \{1 - \exp[-\sin\theta(n_1 - n_3)\gamma_i' R]\} \sin^3\theta d\theta . \tag{12}$$

We use the substitution $u = \sin\theta$ and approximate the integral over u by the Gaussian integration of moments in which the integral

$$\int_0^1 u^k F(u) du = \sum_j \omega_{kj} F(u_j) .$$

The values of u_j and the weighting factors ω_{kj} are given in Ref. 7. We use eight terms to approximate the integrals in Eqs. (11) and (12). The rate equations for n_1 and n_2 become the following:

$$\frac{dn_2}{dt} = -\frac{I_{\bar{\nu}}}{h\nu_{23}} \frac{\lambda_{23}^2}{4\pi} A_3(n_2 - n_3) + A_{32}n_3 - \frac{n_2 - n_1}{T_1} - \frac{A_3n_3}{2\sqrt{\pi}} \sum_i \omega_i \int_0^1 \left[1 - \exp \left[-(n_2 - n_3)\gamma_i R \frac{(2 - u^2)}{u} \right] \right] \frac{(2 - u^2)u du}{(1 - u^2)^{1/2}} \tag{13}$$

$$= \frac{I_{\bar{\nu}}}{h\nu_{23}} \frac{\lambda_{23}^2}{4\pi} A_3(n_2 - n_3) + A_{32}n_3 - \frac{n_2 - n_3}{T_1} - \frac{A_3n_3}{2\sqrt{\pi}} \sum_i \omega_i \sum_j \omega_{1j} \left[\frac{1 - \exp \left[-(n_2 - n_3)\gamma_i R \frac{2 - u_j^2}{u_j} \right]}{(1 - u_j^2)^{1/2}} \right] (2 - u_j^2) \tag{14}$$

and

$$\frac{dn_1}{dt} = A_{31}n_3 + \frac{n_2 - n_1}{T_1} - \frac{A_3n_3}{2\sqrt{\pi}} \sum_i \omega_i \int_0^1 \{1 - \exp[-(n_1 - n_3)\gamma_i' Ru]\} \frac{u^3 du}{(1 - u^2)^{1/2}} \tag{15}$$

$$= A_{31}n_3 + \frac{n_2 - n_1}{T_1} - \frac{A_3n_3}{2\sqrt{\pi}} \sum_i \omega_i \sum_j \omega_{3j} \left[\frac{1 - \exp[-(n_1 - n_3)\gamma_i' Ru_j]}{(1 - u_j^2)^{1/2}} \right] . \tag{16}$$

Even at quite large magnetic fields it is appropriate to use the approximation that $\nu_{23} = \nu_{13} = \nu_0$ and $\lambda_{13} = \lambda_{23} = \lambda_0$ in Eqs. (13)–(16). In this situation $\gamma_i = \gamma_i'$. The rate equations for n_1 and n_2 can be written as

$$\frac{dn_2}{dt} = -\frac{I_{\bar{\nu}}}{h\nu_0} \frac{\lambda_0^2}{4\pi} A_3(n_2 - n_3) + A_{32}n_3 - \frac{n_2 - n_1}{T_1} - n_3 R_{32} \tag{17}$$

and

$$\frac{dn_1}{dt} = A_{31}n_3 + \frac{n_2 - n_1}{T_1} - n_3 R_{31} , \tag{18}$$

where R_{32} and R_{31} are given by

$$R_{32} = K_2 \frac{A_3}{2\sqrt{\pi}} \sum_i \omega_i \sum_j \omega_{1j} \left[\frac{1 - \exp \left[-\gamma_i(n_2 - n_3)R \frac{2 - u_j^2}{u_j} \right]}{(1 - u_j^2)^{1/2}} \right] (2 - u_j^2) \tag{19}$$

and

$$R_{31} = K_1 \frac{A_3}{2\sqrt{\pi}} \sum_i \omega_i \sum_j \omega_{3j} \left[\frac{1 - \exp[-(n_1 - n_3)R\gamma_i u_j]}{(1 - u_j^2)^{1/2}} \right] . \tag{20}$$

It should be noted that R_{32} is a function of $n_2 - n_3$, and R_{31} is a function of $n_1 - n_3$. From the form of R_{32} and R_{31} it is obvious that R_{32} is zero if $n_2 - n_3 = 0$, and R_{31} is zero if $n_1 - n_3 = 0$. Thus, the rate equations approach the correct limit as the population differences go to zero. If $n_2 - n_3$ is infinite then we expect physically that R_{32} equals A_{32} so that the effective decay rate from state 3 into state 2 is zero. Similarly, if $n_1 - n_3$ is infinite, we expect $R_{31} = A_{31}$. Because of the approximations made in evaluating the integrals neither $R_{32}(n_2 - n_3 = \infty)$ is equal to A_{32} nor is $R_{31}(n_1 - n_3 = \infty)$ equal to A_{31} . Even a small error in the high-density limit for R_{32} or R_{31} is very serious for radiation-trapping calculations because it means that the calculated decay rate remains too large. For example, a 10% error in both R_{31} and R_{32} would mean that the calculated radiative decay rate for n_3 would only decrease to about 10% of A_3 rather than decreasing to zero as the density goes to infinity. In order to avoid serious errors in R_{31} and R_{32} at high atomic density, we have introduced the constants K_2 and K_1 in Eqs. (18) and (19). We evaluate K_2 by setting $n_2 - n_3 = \infty$ and finding the value of K_2 to make $R_{32} = A_{32}$, and we evaluate K_1 by setting $n_1 - n_3 = \infty$ and finding the value of K_1 that makes $R_{31} = A_{31}$. If the integrations that lead to the expressions for R_{32} and R_{31} had been done exactly, K_2 and K_1 would have been 1. Because of the approximations in evaluating the integrals, we find that K_1 and K_2 differ from 1. In all cases K_1 and K_2 differ from 1 by less than 0.1.

IV. DISCUSSION OF RESULTS

We note that the state populations and ground-level polarization depend on NR as can be seen from Eqs. (19) and (20). Thus the polarizations we calculate for a given N and $R = 7.5 \times 10^{-3}$ m are identical to the polarizations for different density N' and radius R' provided $N'R' = N \times 7.5 \times 10^{-3}$ m.

We have used Eqs. (17)–(20) together with $N = n_1 + n_2 + n_3$ to make numerical calculations of n_1 , n_2 , and n_3 using the following parameters. The tempera-

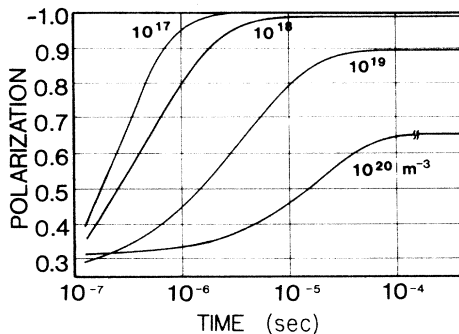


FIG. 2. Polarization as a function of time for different atomic densities N . The optical pumping begins with zero polarization at time $t=0$. Here we have taken the pumping intensity per unit frequency I_{ν} to be 2.85×10^{-6} W/m² Hz and the ground-level relaxation time T_1 to be 150 μ s. A break in the scale for the atomic density of 10^{20} atoms/m² is made to show the steady-state polarization for that density.

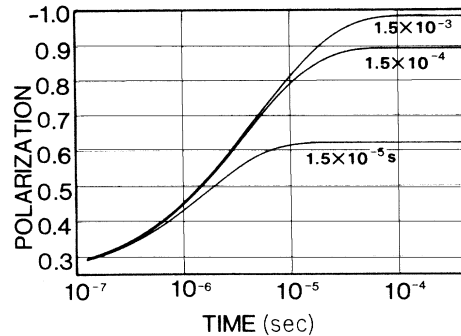


FIG. 3. Polarization as a function of time for different ground-level relaxation times T_1 . The optical pumping begins with zero polarization at time $t=0$. These results are for pumping intensity per unit frequency I_{ν} of 2.85×10^{-6} W/m² Hz and atomic density N of 10^{19} atoms/m².

ture of the target is taken as $T=600$ K, the radius of the target is taken as $R=7.5 \times 10^{-3}$ m, the mass of the alkali-metal atom is $M=23u$, the wavelength of the resonance radiation is $\lambda_0=589$ nm, and the untrapped decay rate of the excited state is $A_3=6.1 \times 10^7$ sec⁻¹. These parameters are those appropriate for the Na vapor target used in the optically pumped H⁻ ion source described later in this section.⁸⁻¹⁰

We show selected calculations on several graphs. Figures 2 and 3 show the time dependence of the ground-level electron-spin polarization P , assuming the polarization is zero at the time $t=0$. The electron-spin polarization is defined as

$$P = (n_2 - n_1) / (n_2 + n_1).$$

The relaxation time T_1 and the light intensity I are treated as parameters. As expected for σ^- pumping light, the polarization as a function of the time decreases from its initial value of 0 toward its steady-state value. The steady-state value of the polarization is given by

$$P = -1 / \left[1 + \frac{2}{T_1(A_{31} - R_{31})} \left(1 + \frac{A_3 - R_{32} - R_{31}}{\alpha} \right) \right], \quad (21)$$

where $\alpha = I_{\nu} \lambda_0^2 A_3 / 4\pi$. If we had used σ^+ rather than σ^- polarization, then the sign of the polarization would be + rather than -. The approach to the steady-state polarization depends on both the laser intensity and the radiation trapping produced by the ground-level atoms in states 1 and 2.

The steady-state polarization as given in Eq. (21) is rather complicated to calculate because one must calculate the radiation-trapping terms R_{32} and R_{31} for the steady-state atomic densities n_1 , n_2 , and n_3 . In Table I we present the steady-state polarization as a function of the intensity of the pumping light with the total density and the relaxation time treated as parameters. It is important to note that even when the optical pumping light intensity per unit frequency becomes infinite, the electron-spin polarization of the optically pumped alkali-metal vapor does not become large unless the spin-relaxation time T_1 is longer than the radiation-trapped decay time from the ex-

TABLE I. Steady-state polarizations reached as a function of the ground-state relaxation time T_1 and the total atomic density N . The cases shown are for a pumping intensity per unit frequency I_ν of 7.13×10^{-7} W/m² Hz, 2.85×10^{-6} W/m² Hz, 1.14×10^{-5} W/m² Hz, and ∞ . These correspond to laser powers of $\frac{1}{4}$ W, 1 W, 4 W, and ∞ , respectively, evenly distributed over the cross-sectional area of the cylinder and over the frequency bandwidth $g(0)^{-1}$ which is nearly the Doppler linewidth.

	N (m ⁻³)	I_ν (W/m ² Hz)			
		7.13×10^{-7}	2.85×10^{-6}	1.14×10^{-5}	∞
$T_1 = 1.5$ ms	10^{17}	0.998	0.9996	0.9998	0.99992
	10^{18}	0.995	0.998	0.9993	0.9996
	10^{19}	0.958	0.979	0.989	0.993
	10^{20}	0.899	0.913	0.920	0.929
$T_1 = 150$ μ s	10^{17}	0.986	0.996	0.998	0.9992
	10^{18}	0.956	0.985	0.993	0.996
	10^{19}	0.841	0.890	0.918	0.940
	10^{20}	0.636	0.657	0.667	0.681
$T_1 = 15$ μ s	10^{17}	0.882	0.961	0.984	0.992
	10^{18}	0.770	0.889	0.941	0.964
	10^{19}	0.555	0.622	0.664	0.708
	10^{20}	0.281	0.301	0.312	0.326

cited state 3 to the ground state 1, $(A_{31} - R_{31})^{-1}$. In fact, for $I = \infty$ we find

$$P = -1/[1 + 2/T_1(A_{31} - R_{31})].$$

There is interest in producing polarized alkali-metal targets. For example, a current use for an electron-spin-polarized alkali target is in the optically pumped polarized H⁻ ion source.⁸⁻¹⁰ In the optically pumped polarized H⁻ ion source, H⁺ ions are incident on an optically pumped polarized Na vapor target, which is in a high magnetic field. The H⁺ ions pick up a polarized electron in the optically pumped target, forming electron-spin-polarized fast H⁰ atoms. The polarization of the electron is transferred to the nucleus, and some of the fast H⁰ atoms are converted into polarized H⁻ ions in a second

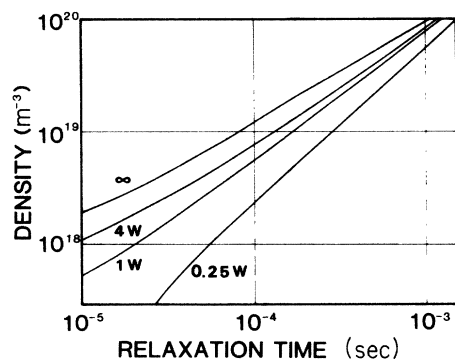


FIG. 4. The maximum density which may be optically pumped to a polarization of 0.9 as a function of the ground-level relaxation time T_1 . The cases of pumping intensity per unit frequency I_ν equaling 7.13×10^{-7} W/m² Hz, 2.85×10^{-6} W/m² Hz, 1.14×10^{-5} W/m² Hz, and the limit of infinite intensity are shown. These correspond to laser powers of $\frac{1}{4}$ W, 1 W, 4 W, and ∞ , respectively, evenly distributed over the cross-sectional area of the cylinder and over the frequency bandwidth $g(0)^{-1}$ which is nearly the Doppler linewidth.

alkali-metal target. One limitation on the density and polarization of the optically pumped Na target is radiation trapping. For example, if we require an electron-spin polarization of 0.9 then we can estimate the radiation-trapping limit to the density for a given relaxation time. The results of such a calculation are given in Fig. 4. For a sodium vapor target, relaxation times corresponding to 10–15 wall bounces have been obtained using a fluorocarbon rubber wall coating.¹¹ This corresponds, for our geometry, to 150 μ s. With this relaxation time, optically pumped Na vapor targets in a high magnetic field can have polarizations of greater than 90%, even for a vapor as dense as 10^{19} atoms/m³. For other alkali-metal vapors, such as Rb, walls with even longer relaxation times are known so that these vapors may be useful as an optically pumped target at even higher density than Na.¹

Finally we would like to discuss the limitations imposed by the approximations made in our calculations. First we can comment on the numerical approximations that result from using the Hermite integration and the Gaussian integration of moments. We have tested the accuracy of these integrations in a number of ways. We have used these methods to evaluate integrals of exactly integrable functions similar to those we approximate, and we find results that in all cases are accurate to a few percent. We have also integrated a few of the functions we use by very accurate numerical methods and again find that our results differ from more precise calculations by only a few percent.

In our calculations we have used densities up to 10^{20} atoms/m³ and have used the Doppler line shape. Collisions alter and broaden the line shape. This effect becomes important for densities of about 5×10^{19} atoms/m³. The increase in the line shape due to collisions reduces the radiation trapping from that which we calculate. Thus, we believe that our values of the polarization for densities above 5×10^{19} atoms/m³ represent a lower limit to the polarization.

Probably the most serious approximation introduced in our calculations is the approximation that n_1 , n_2 , and n_3 are independent of the position in the target. For ground-state relaxation times that correspond to several flight times across the target, it is reasonable to believe that the ground-level densities n_1 and n_2 do not depend strongly on the radial position in the target. The approximation that the excited-state density n_3 is independent of the radial position in the alkali-metal vapor is, however, suspect. Radiation emitted near $r=R$ has a higher probability of escaping the alkali-metal vapor than radiation emitted near $r=0$, so one expects n_3 to be larger near the axis of the cylinder. In order to determine the effect of our assumption, we have calculated radiation-trapped polarization for a Na vapor with n_3 independent of position r and with n_3 arbitrarily being forced to have a spatial variation $\cos(\pi r/2R)$, consistent with the density going to zero at $r=R$. We find that the steady-state polarization achieved when n_3 varies as $\cos(\pi r/2R)$ differs from the polarization when n_3 is independent of r by less than 20% for total densities of 10^{19} atoms/m³. Thus our approximation that n_3 is independent of position probably introduces uncertainties of about 20% into our calculations at the total densities less than 10^{19} atoms/m³.

A final approximation we made was that the alkali-metal atom has no nuclear spin. In a high magnetic field the nuclear spin is decoupled from the electron spin. One might incorrectly infer that this is the same as assuming that the alkali-metal atom has no nuclear spin. In order to understand the effect of a nuclear spin, let us consider the situation for a particular alkali-metal atom ²³Na. The nuclear spin of ²³Na is $\frac{3}{2}$. The ground-level hyperfine separation (HFS) in ²³Na is $\Delta\nu_{\text{HFS}}=1.77 \times 10^9$ Hz. The Doppler width of ²³Na at $T=600$ K is $\Delta\nu_D=1.7 \times 10^9$ Hz (full width at half maximum). In a high magnetic field the ground level of ²³Na has eight states specified by the various values of m_S and m_I , the z components of the electron spin and the nuclear spin. Each of the four states with $m_S=\frac{1}{2}$ is separated from the nearest state by

$\Delta\nu_{\text{HFS}}/4=443$ MHz. The absorption of σ^- light by an atom in the $^2S_{1/2}$ state with $m_S=\frac{1}{2}, m_I$ produces an atom in the $^2P_{1/2}$ level with $m_J=-\frac{1}{2}, m_I$. This absorption has a Doppler width $\Delta\nu_D$. The total absorption profile for the $^2S_{1/2}$ level by σ^- light has a width of about

$$\Delta\nu = \frac{3}{4} \Delta\nu_{\text{HFS}} + \Delta\nu_D = 3 \times 10^9 \text{ Hz} .$$

Since this line is wider than the Doppler width used in our calculations, our calculations overestimate the effect of radiation trapping. Thus the estimates in Table I of densities at which a polarization of 90% can be obtained are lower limits and densities about up to a factor of 2 larger can actually be optically pumped to a polarization of 90% with very high light intensity.

We assume that the light intensity is constant through the optically pumped sample. The accuracy of this assumption depends on the thickness (in atoms/cm²) of the alkali-metal vapor target. It is possible to easily envision situations where this is accurate. Even if this is not accurate for the vapor target, it may be accurate for segments of the target, and the polarization at given points in the target can then be estimated segment by segment. Finally, we caution that our calculations are certainly *not* valid at low fields where light emitted by one transition, λ_{ij} , can be absorbed by another transition, λ_{kl} .

In conclusion, high polarizations can be obtained when the radiation-trapped decay rate of the excited state into the highly populated ground state $A_{31}-R_{31}$ exceeds the ground-state relaxation rate T_1^{-1} . We estimate that at the present time it is possible to produce alkali-metal targets with electron-spin polarization greater than 90% and density greater than 10^{19} atoms/m³ in a cylindrical geometry with radius 7.5×10^{-3} m.

ACKNOWLEDGMENTS

We acknowledge the partial support of this research by the United States Department of Energy.

¹W. Happer, Rev. Mod. Phys. **44**, 169 (1972).

²E. A. Milne, J. London Math. Soc. **1**, 1 (1926).

³T. Holstein, Phys. Rev. **72**, 1212 (1947).

⁴C. van Trigt, Phys. Rev. **181**, 97 (1969).

⁵J. P. Barrat, J. Phys. Radium **20**, 541 (1959).

⁶M. I. D'Yakanov and V. I. Perel', Zh. Eksp. Teor. Fiz. **47**, 1483 (1964) [Sov. Phys.—JETP **20**, 997 (1965)].

⁷M. Abramowitz and I. A. Stegun, *Handbook of Mathematical Functions with Formulas, Graphs, and Mathematical Tables*

(Dover, New York, 1970), Chap. 7.

⁸L. W. Anderson, Nucl. Instrum. Methods **167**, 363 (1979).

⁹L. W. Anderson, IEEE Trans. Nucl. Sci. **NS-30**, 1051 (1983).

¹⁰Y. Mori, K. Ikegami, Z. Igarashi, A. Takagi, and S. Fukumoto, in *Proceedings of the Conference on Polarized Proton Ion Sources, TRIUMF, Vancouver, 1983*, edited by G. Roy and P. Schmor (AIP, New York, 1984), pp. 123-132.

¹¹D. R. Swenson and L. W. Anderson, Nucl. Instrum. Methods **B12**, 157 (1985).